

# Automated Batch Distillation Process Simulation for a Large Hybrid Dataset for Deep Anomaly Detection

Jennifer Werner<sup>\*1</sup>, Justus Arweiler<sup>\*2</sup>, Indra Jungjohann<sup>\*2</sup>, Jochen Schmid<sup>\*1</sup>, Fabian Jirasek<sup>2</sup>, Hans Hasse<sup>2</sup>, and Michael Bortz<sup>1</sup>

<sup>1</sup>Fraunhofer Institute for Industrial Mathematics (ITWM), Kaiserslautern, Germany

<sup>2</sup>Laboratory of Engineering Thermodynamics (LTD), RPTU Kaiserslautern, Germany

## Abstract

Anomaly detection (AD) in chemical processes based on deep learning offers significant opportunities but requires large, diverse, and well-annotated training datasets that are rarely available from industrial operations. In a recent work, we introduced a large, fully annotated experimental dataset for batch distillation under normal and anomalous operating conditions. In the present study, we augment this dataset with a corresponding simulation dataset, creating a novel hybrid dataset. The simulation data is generated in an automated workflow with a novel Python-based process simulator that employs a tailored index-reduction strategy for the underlying differential-algebraic equations. Leveraging the rich metadata and structured anomaly annotations of the experimental database, experimental records are automatically translated into simulation scenarios. After calibration to a single reference experiment, the dynamics of the other experiments are well predicted. This enabled the fully automated, consistent generation of time-series data for a large number of experimental runs, covering both normal operation and a wide range of actuator- and control-related anomalies. The resulting hybrid dataset is released openly. From a process simulation perspective, this work demonstrates the automated, consistent simulation of large-scale experimental campaigns, using batch distillation as an example. From a data-driven AD perspective, the hybrid dataset provides a unique basis for simulation-to-experiment style transfer, the generation of pseudo-experimental data, and future research on deep AD methods in chemical process monitoring.

## 1 Introduction

In chemical engineering, early and reliable anomaly detection (AD) is essential for the safe operation of plants and for preventing failures and accidents. Beyond substantial economic losses, undetected anomalies may pose serious risks to human health and the environment. Industrial chemical processes are monitored by a wide range of sensors that generate diverse multivariate time-series data, which are processed by plant control systems. Although these systems incorporate automated AD functionalities, decision-making still largely relies on the expertise of experienced operating personnel [1–5].

Machine learning (ML) provides promising new approaches for enhancing AD in chemical processes [6–16]. However, the development of such methods requires extensive datasets for training and validation and was, until recently, hindered by the lack of suitable data, the only openly available chemical process data being simulation data for the fictitious Tennessee Eastman process [7, 17, 18]. Only recently have datasets from real chemical processes been published, specifically generated to support ML-based AD, including data from a laboratory-scale batch distillation

---

<sup>\*</sup>These authors contributed equally to this work.

plant [19] and a continuous distillation mini-plant [20]. Both datasets are accompanied by rich metadata, including comprehensive plant descriptions, and comprise fault-free experiments as well as corresponding anomalous runs with thorough annotations. These datasets were created at universities within the DFG Research Unit “Deep Learning on Sparse Chemical Process Data.” In cooperation with this Research Unit, BASF SE also disclosed data from an industrial process; however, this dataset provides substantially less metadata and annotations than the academic datasets. All three datasets were published in the 2025 NeurIPS Datasets and Benchmarks track [21].

Despite this recent progress, the systematic collection of experimental data for the development, training, and validation of AD methods remains highly challenging. In particular, suitably annotated and labeled data from real processes will remain scarce, not only because producing such data is effort-intensive. Industrial processes are designed to operate safely and stably, and deviations from normal operation are both rare and undesirable. Consequently, historical plant data – if accessible at all – are typically strongly imbalanced, dominated by normal operation with only a few anomalous events that are often incompletely documented. Moreover, deliberately inducing anomalous operating conditions in experimental or industrial settings is generally unacceptable for safety, regulatory, and economic reasons [22, 23].

Process simulation, therefore, constitutes an attractive complementary data source, as it enables the systematic, reproducible, and scalable generation of process data across a wide range of operating conditions, including controlled variations and well-defined anomalous scenarios. At the same time, simulation data alone are insufficient to fully capture the complexity, variability, and noise characteristics of real process data, limiting their direct applicability to data-driven AD. These considerations motivate hybrid data strategies that combine the coverage and controllability of simulations with the realism of experimental data, aiming to leverage the strengths of both worlds.

We consider batch distillation as a representative example of an instationary chemical process to investigate how dynamic process simulation can support the development of AD methods. Our objective is to generate simulation data for all 119 batch distillation experiments reported in [19, 21] in a fully consistent and automated manner. Achieving this requires developing a dedicated simulation workflow, with a central element: a suitable dynamic process simulation engine.

It is well known that the robust simulation of batch distillation processes is challenging, as it requires the solution of nonlinear differential-algebraic equations with a (differentiation) index of at least 2 [24–27]. Accordingly, a wide range of dedicated numerical solution strategies have been developed to solve these equations [28–45]. In the present work, we build on a recently developed Python-based simulation tool [45], which establishes and exploits a novel index-reduction approach and enables the robust and fully automated generation of batch distillation simulation data under diverse operating conditions. Compared to the simulation model from [45], only minor extensions had to be made to reflect the specifics of the concrete batch distillation plant considered here.

We leverage the thus extended simulation engine to generate data that correspond directly to the experimental records reported in [19, 21] and to augment them, in particular by providing information that is inaccessible in the experiments. Together, the experimental and simulation datasets form a unique hybrid dataset that is directly suitable for the development and benchmarking of AD methods. To the best of our knowledge, this dataset represents the largest collection of consistent experimental and simulation data for dynamic chemical processes currently available.

In the present study, we address the forward problem of generating simulation data from existing experimental data. However, the corresponding inverse problem – the generation of pseudo-experimental data from simulation data – is at least equally fascinating. Solving this problem would enable the creation of large, diverse datasets, including those with difficult, unsafe, or undesirable operating conditions, supporting the development of ML-based AD methods. The hybrid dataset introduced here provides a valuable foundation for tackling this inverse problem, for example, through approaches based on style transfer [46–49].

To simulate the experiments from the large dataset [19, 21], a suitable workflow had to be established. In a first

step, the general plant-specific model parameters, such as the number of theoretical stages per meter and thermal capacities, were fixed. For some plant-specific parameters, this was done a priori based on available metadata for the plant. For a subset of plant-specific parameters, an adjustment was made to a single representative experiment. In a second step, the other experiments were simulated, keeping the general parameters constant. The experiment-specific parameters were adopted from the database, and no further adjustments were made, so these simulations are predictions. Hence, this corresponds to splitting the experimental dataset into a training set containing a single experiment and a test set containing the remaining 118 experiments. Of those 118 experiments, 4 exhibit liquid-liquid equilibria (LLE), which are not accounted for in the current simulation model. The convergence of these simulations covering different mixtures, feed compositions, and operating conditions is not trivial. Furthermore, anomalies had to be predicted. Doing this is straightforward for anomalies introduced by perturbing the control parameter setpoints in the simulation. Anomalies stemming from other perturbations, such as the addition of foaming agents or the corruption of sensor data (e.g., due to noise or drift), could not be simulated, as these effects are not covered by the simulation model. In these cases, the simulations covered only the unperturbed phases of the experiment. To implement an automated workflow, a standardized procedure for assessing the quality of predictions had to be established.

The simulation results obtained in the present work are released openly together with detailed simulation metadata and comprehensive annotations, following the ontology of the experimental database [19]. Technically, the simulation and experimental datasets are merged into a single hybrid database that contains both data types for 115 experiments, including 36 of the 71 confirmed anomalies described in [19]. This unique hybrid dataset provides rich opportunities for future research on AD in chemical processes.

## 2 Experimental data

The simulation model developed in this work describes experiments carried out with a batch distillation plant, namely, a modified version of the Iludest LM 2/S glass plant, consisting of a 2 L reboiler vessel and a 1.5 m-high DN30 column section with DX structured packing (Sulzer AG). The piping and instrumentation (P&I) diagram of the plant is given in Fig. 1. In the experiments, the plant was operated in a static control regime, with fixed constant operating points for pressure, heat supply, and reflux ratio. The initial composition and mass of the feed mixture are known and reported in the database. For a detailed description of the plant and its operation, the reader is referred to [19].

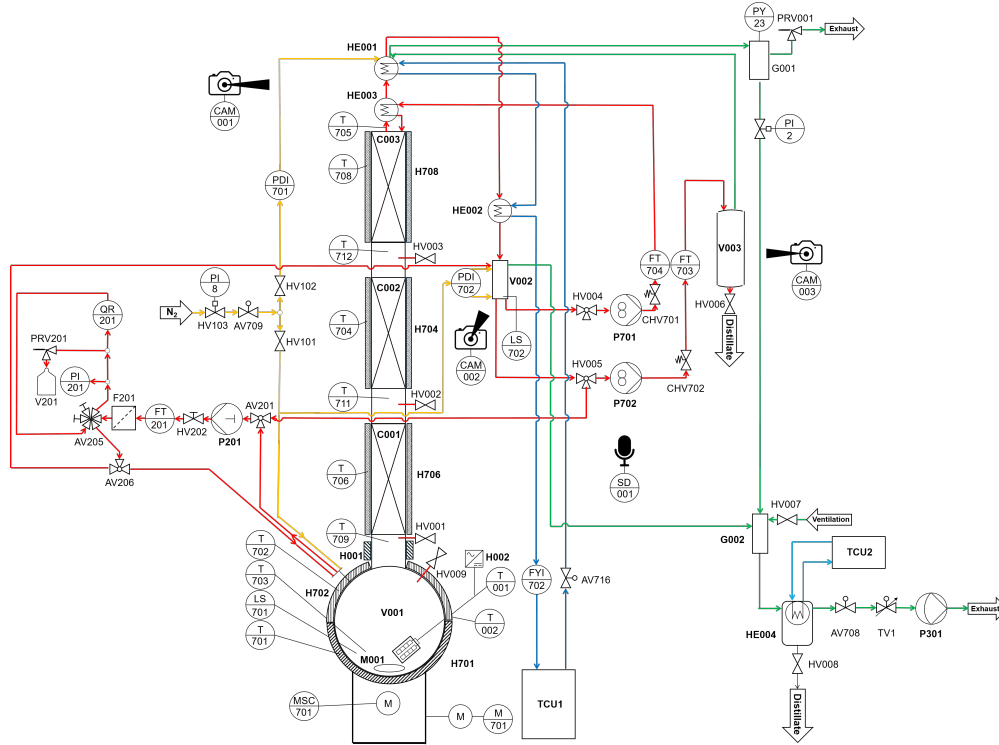


Figure 1: P&I diagram of the laboratory batch distillation plant. Color code of the lines: product (red), cooling water (dark blue), cooling ethanol (light blue), nitrogen (yellow), and pressure control (green). The equipment list in which the labels are declared is described in [19].

In this work, only the operating phase of the experiments is considered; the start-up and shut-down phases are disregarded. In the batch distillation experiments, anomalies were deliberately introduced by perturbing the process. All anomalies in the distillation processes in the database are described in a comprehensive metadata scheme [19], allowing the deduction of the underlying perturbations as adjustments to the time-dependent simulation control parameters. Apart from the start and end time of the applied perturbation, information on the perturbation itself, as well as the affected part of the plant, is available. For the full documentation, the reader is referred to [19, 21].

### 3 Simulation model

In this section, we introduce the simulation model used to capture the dynamic behavior of the batch distillation plant. Specifically, we spell out the assumptions underlying the model (Section 3.1) and the model’s state variables and control parameters (Section 3.2). In Section 3.3, we then explain how the simulation model from [45] was extended in order to represent the experimental data obtained with the plant described in Section 2. Finally, we explain how the plant-specific model parameters and the experiment-specific control parameters were set for the various simulations performed to create the hybrid dataset (Section 3.4).

#### 3.1 Assumptions

As most papers on the simulation of batch distillation processes, such as [28, 29, 33–37, 39, 40, 42–44], we use an equilibrium-stage model for the distillation column and describe the temporal evolution of the distillation process by means of the mass and energy balances around the equilibrium stages and by means of phase equilibrium conditions and the summation equations for the individual equilibrium stages. Specifically, we consider batch distillation processes in columns with  $S \geq 2$  stages for multi-component mixtures consisting of  $C \geq 2$  components. Stage 1

is the heated reboiler vessel, and stage  $S$  is the head, which is connected to a condenser. The condenser, in turn, is connected to a buffer vessel  $B$ , where the condensed product is gathered, before it is either returned to the column as reflux or withdrawn as distillate. In [45], we did not consider such a buffer vessel. However, it turned out that incorporating the buffer vessel into the model substantially improved the simulation-experiment fits across the diverse operating and initial conditions covered by the experimental database underlying the present paper. A schematic of the batch distillation column model is shown in Figure 2.

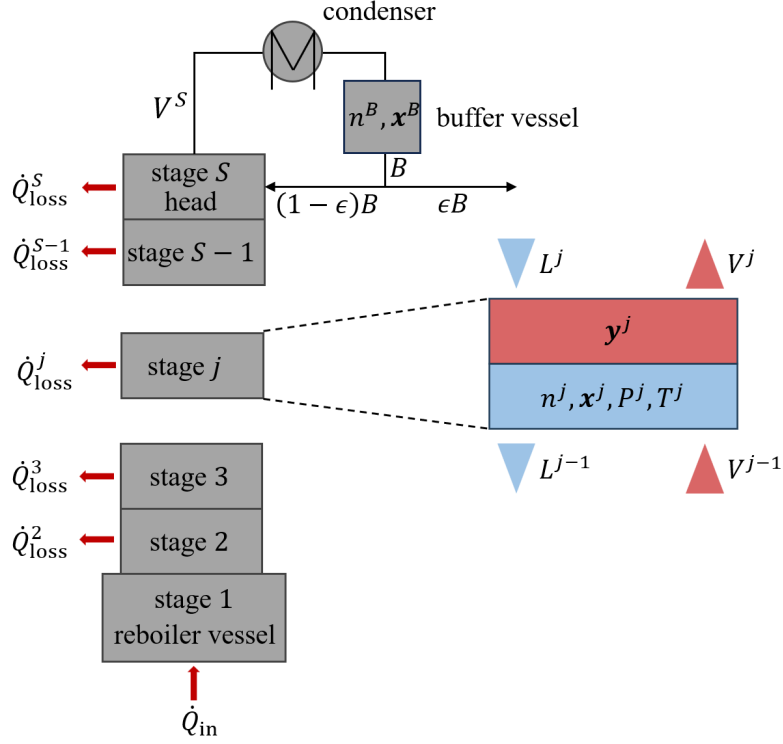


Figure 2: Schematic of the considered batch distillation column model. Symbols are explained in the main text.

As in [45], it is assumed that

- (i) the vapor holdup on all stages can be neglected,
- (ii) there is total condensation in the condenser,
- (iii) phases do not disappear, i.e., that exactly two phases are in equilibrium with each other, namely one vapor and one liquid phase, on all stages at all times.

Additionally, the mass in the buffer vessel after the condenser is constant in time. Apart from this buffer vessel, we made the following additional changes to the simulation model described in [45]:

- (i) The internal energy  $U_{\text{mat}}^j$  stored in the packing material of stage  $j$  and in the walls around stage  $j$  is given by

$$U_{\text{mat}}^j = c^j (m_{\text{steel}}^j c_p^{\text{steel}} + m_{\text{glass}}^j c_p^{\text{glass}}) (T^j - T^{\text{ref}}), \quad (1)$$

where  $c_p^{\text{steel}}$  and  $c_p^{\text{glass}}$  are the heat capacities of the employed steel packing and glass walls, respectively, while  $m_{\text{steel}}^j$  and  $m_{\text{glass}}^j$  are the masses of steel packing and the glass walls on or around stage  $j$ , respectively. Furthermore,  $T^j$  is the temperature at stage  $j$ ,  $T^{\text{ref}}$  is a reference temperature for the heat capacities, and

the parameters  $c^j$  are adjustable correction factors that need to be calibrated to data from the specific plant under consideration.

- (ii) There are heat losses  $\dot{Q}_{\text{loss}}^j$  from each column stage  $j \in \{2, \dots, S\}$  and these are constant in time.
- (iii) The condenser temperature  $T^{\text{cond}}$  is regulated such that, at all times, it is a constant  $\Delta T$  below the head temperature  $T^S$ . In short,

$$T^{\text{cond}} = T^S - \Delta T. \quad (2)$$

- (iv) The pressure on each stage  $j$  is described as follows in the simulation model:

$$P^j = P^S + (S - j) \frac{\Delta P}{S - 1} \quad (j \in \{1, \dots, S\}), \quad (3)$$

where  $P^j$  denotes the pressure on stage  $j$  and  $\Delta P$  denotes the total pressure drop from the reboiler vessel to the column head.

### 3.2 Variables

The state of the considered distillation process is completely described by the following variables:

- $n^j$ : liquid mole holdup on stage  $j \in \{1, \dots, S\}$ ,
- $n^B$ : liquid moles in the buffer vessel,
- $\mathbf{x}^j = (x_1^j, \dots, x_C^j)$ : liquid molar composition on stage  $j \in \{1, \dots, S\}$
- $\mathbf{x}^B = (x_1^B, \dots, x_C^B)$ : liquid molar composition in the buffer vessel,
- $\mathbf{y}^j = (y_1^j, \dots, y_C^j)$ : vapor molar composition on stage  $j \in \{1, \dots, S\}$ ,
- $T^j$ : temperature on stage  $j \in \{1, \dots, S\}$ ,
- $L^j$ : liquid molar downstream from stage  $j + 1$  to stage  $j$ ,
- $V^j$ : vapor molar upstream from stage  $j$  to stage  $j + 1$ ,
- $B$ : liquid molar stream going out of the buffer vessel,
- $D$ : molar distillate stream.

Note that  $D = \epsilon B$ , where  $\epsilon$  is the efflux ratio defined below. Furthermore, the apparatus holdup is defined as follows:

$$n^{\text{app}} := n^1 + \dots + n^S + n^B. \quad (4)$$

The values of the following control (input) parameters as functions of time have to be specified:

- $\epsilon$ : the efflux ratio

$$\epsilon := D/B \in [0, 1] \quad (5)$$

being defined as the share of the liquid stream  $B$  that is withdrawn from the column,

- $P^S$ : the pressure on the head stage  $S$ ,
- $\Delta P$ : the pressure drop from the reboiler vessel to the head stage  $S$ ,
- $\dot{Q}_{\text{in}}$ : the reboiler heat duty.

### 3.3 System equations

Compared to [45], the system equations had to be extended as follows:

- the total and component-wise mass balances around the buffer vessel were added to the system,
- the energy balances were extended by the internal energy  $U_{\text{mat}}^j$  stored in the packing material and the walls of the corresponding stage, and the heat losses  $\dot{Q}_{\text{loss}}^j$ ,
- an equation ensuring the mass constancy in the buffer vessel was added.

This system of equations is spelled out in the Supporting Information.

### 3.4 Choice of the model and control parameter values

In this section, we discuss how the simulation parameters were set to represent the laboratory batch distillation plant. We distinguish between plant- and experiment-specific parameters. The plant-specific parameters apply only to the plant and are thus the same across all experiments. On the other hand, several parameters are experiment-specific and must be set individually for each experiment according to the available experimental data. This distinction is described in more detail below.

#### 3.4.1 Plant-specific parameters

The plant-specific parameters are

- the number of stages  $S$ ,
- the heat loss  $\dot{Q}_{\text{loss}}^j$  on each stage  $j$ ,
- the temperature difference  $\Delta T$  between the head and the condenser stage,
- the heat capacities of the plant equipment, here the heat capacities  $c_p^{\text{steel}}$  and  $c_p^{\text{glass}}$  of steel and glass, and the masses of the plant equipment, here the masses  $m_{\text{steel}}^j$  and  $m_{\text{glass}}^j$  of steel and glass on each stage  $j$ ,
- and the correction parameters  $c^j$  in the model (1).

These parameters were set once and then fixed for all experiments:

The number of stages is  $S = 12$  for each simulation run. This value was determined from measurements of the number of theoretical stages per meter (NTSM) using a binary test-mixture of (ethanol + 2-propanol); details are provided in Supporting Information.

The column of the laboratory distillation plant is insulated (heating elements are installed along the column to minimize heat losses), while the column head is not insulated. Accordingly, in the simulation model, we assumed no heat losses in the column stages and a small heat loss of 2 W at the top of the column:

$$\dot{Q}_{\text{loss}}^2 = \dots = \dot{Q}_{\text{loss}}^{S-1} := 0 \text{ W} \quad \text{and} \quad \dot{Q}_{\text{loss}}^S := 2 \text{ W}. \quad (6)$$

Concerning the temperature offset  $\Delta T$  between the head and the condenser stage (Assumption 3 (iii)), we assumed

$$\Delta T := 20 \text{ K}. \quad (7)$$

To model the thermal inertia of the plant as in (1), masses and heat capacities of the plant equipment must be known. The reboiler vessel, including heating elements and insulation, has a mass of  $m_{\text{glass}}^1 = 1.25 \text{ kg}$ , the insulation and the submerged heating rod account for a combined mass of  $m_{\text{steel}}^1 = 0.25 \text{ kg}$ , which was determined gravimetrically. In contrast, the masses of glass and structured packing on the theoretical separation stages cannot be measured gravimetrically and were estimated to be  $m_{\text{glass}}^j = 0.2 \text{ kg}$  and  $m_{\text{steel}}^j = 0.058 \text{ kg}$  for all  $j \in \{2, \dots, S\}$ . The glass material used in the plant is borosilicate-glass with a heat capacity of  $c_p^{\text{glass}} = 830 \text{ Jkg}^{-1}\text{K}^{-1}$  [50]. The structured packing, as well as the heating rod, is made from alloy 1.4404 316L with a heat capacity of  $c_p^{\text{steel}} = 510.79 \text{ Jkg}^{-1}\text{K}^{-1}$  [51]. Furthermore, we set the reference temperature  $T^{\text{ref}} = 273.15 \text{ K}$ .

To obtain the correction parameters  $c^j$ , cf. Eq. (1), an adjustment to a single representative experiment was performed. Calibrating them to a single experiment (see Table 1), we found the values

$$c^1 := 1, c^2 = 2.5, \dots, c^S := 2.5 \quad (8)$$

to be appropriate for the plant considered here.

### 3.4.2 Experiment-specific parameters

Each experiment was conducted at a unique operating point; therefore, the experiment-specific parameters must be set individually. These parameters were determined partly from the plant control settings and partly from the measurement data. In our case, the experiment-specific parameters are

- the pressure at the column head  $P^S$  and the pressure drop  $\Delta P$ ,
- the heat duty  $\dot{Q}_{\text{in}}$  applied to the reboiler,
- and the efflux ratio  $\epsilon$ .

The pressure  $P^S$  for each experiment was set equal to the setpoint head pressure  $P^{\text{set}}$ , and the pressure drop  $\Delta P$  was determined from the experimentally observed pressure drop. The pressures  $P^j, j \in \{1, \dots, S-1\}$  were then determined by the simple linear pressure drop model given in Eq. (3).

The reboiler heat duty  $\dot{Q}_{\text{in}}$  for each experiment was determined according to

$$\dot{Q}_{\text{in}} = \dot{Q}_{\text{in}}^{\text{set}} - \dot{Q}_{\text{loss}}^{\text{reboiler}} \quad (9)$$

where  $\dot{Q}_{\text{in}}^{\text{set}}$  is the setpoint heat flux and  $\dot{Q}_{\text{loss}}^{\text{reboiler}}$  is the reboiler heat loss, which is modeled as explained in the Supporting Information.

Consistent with the constant-reflux control strategy implemented in the laboratory batch distillation plant (Section 2), the efflux ratio  $\epsilon$  was set to a constant value in all simulations from Section 4 (except when it was perturbed as in Section 4.4.1, of course). This value was determined by averaging the experimentally observed reflux ratio values over the experimental time horizon.

## 4 Results and discussion

### 4.1 Overview

Using the general simulation model introduced in Section 3, we simulated all experiments performed with the batch distillation plant described in Section 2, except for runs exhibiting liquid–liquid equilibria (LLE). This section presents five representative cases: the calibration experiment (Section 4.2), one fault-free experiment (Section 4.3), and three anomalous experiments (Section 4.4). Section 4.5 describes the hybrid dataset established in this work. The experimental batch distillation database [19, 21] documents the anomalies and their physical causes in detail. As outlined in Section 2, anomalies can be represented in the model as time-dependent modifications of control signals, provided their causes are known and correspond to actuator setpoint changes. Perturbations in pressure, heating or cooling duties, condenser operation, efflux ratio, leakage, or material withdrawal can thus be mimicked. In contrast, anomalies affecting fluid dynamics, mixture properties (e.g., addition of foaming agents), or the control regime (e.g., sensor noise or drift) cannot be mapped onto model control parameters. These cases are therefore not included.

For the anomalies considered here, the model requires only (i) the start time of the perturbation, (ii) the time of its removal, and (iii) the modified setpoint value. Transitions were implemented as linear ramps to ensure numerical stability and to reflect experimentally observed rates of change. The three anomalous runs discussed here involve perturbations in the efflux ratio, heat duty, and system pressure.

Experiment identifiers, experiment-specific parameters, and initial conditions at simulation start time  $t_{\text{start}} = 0$  are listed in Table 1. Results for three additional fault-free experiments are given in the Supporting Information. For all experiments, detailed comparisons between simulation and measurement are included in the published hybrid dataset.

Table 1: Experiment-specific parameters, initial conditions  $\mathbf{x}^1(t_{\text{start}} = 0)$  and  $n^{\text{app}}(t_{\text{start}} = 0)$ , and assignment of the experiments discussed here to the database. All experiments are from the folder containing the results for the system (butan-1-ol + propan-2-ol + water). Entries marked with a dagger ( $\dagger$ ) were perturbed in the simulation.

Case	ID	$\dot{Q}_{\text{in}} / \text{W}$	$P^S / \text{Pa}$	$\Delta P / \text{Pa}$	$\epsilon$	$\mathbf{x}^1(0) / \text{mol/mol}$	$n^{\text{app}}(0) / \text{mol}$
Calibration	1	230.71	70000	93.0	0.30	(0.429, 0.43, 0.141)	24.62
Fault-free	2	79.77	70000	75.0	0.44	(0.454, 0.394, 0.152)	17.85
Efflux anomaly	3	79.86	60000	64.0	0.30 $\dagger$	(0.348, 0.433, 0.219)	18.38
Heat duty anomaly	4	77.51 $\dagger$	70000	72.0	0.45	(0.442, 0.431, 0.127)	24.61
Pressure anomaly	5	183.90	50000 $\dagger$	82.0	0.17	(0.276, 0.482, 0.242)	19.59

### 4.2 Calibration experiment

The batch distillation model was calibrated using normal-operation data from a single experiment with the ternary system (1-butanol + 2-propanol + water). The chosen operating point was a moderate one with respect to pressure, reflux ratio, heat duty, and feed composition, avoiding extreme conditions. The experiment was run until the reboiler vessel was depleted and the plant was shut down. Figure 3 shows the comparison between simulation and experiment. Overall, the model captures the main behavior of the process well. In panel a), the simulated temperatures in the reboiler and at the top of the column match the experimental trends and absolute values reasonably closely. The rise in head temperature during the batch is correctly described, though the final increase occurs too early in the simulation. This is likely caused by the simplified treatment of heat losses and holdup.

Panels b) and c) show the liquid molar compositions in the reboiler and buffer vessel. Here, the agreement is also good: the model reproduces the dominant trends and the coupling between both vessels.

In panel d), the simulated distillate and reflux streams are in reasonable agreement with the measurements. The shift between operating regimes occurs earlier and more strongly in the simulation, in line with the earlier temperature rise seen in panel a). Nevertheless, the overall changes in flow rates and their relative magnitudes are represented well. The remaining differences likely arise from simplified fluid-dynamic and control descriptions in the model, as well as uncertainty in the flow measurements.

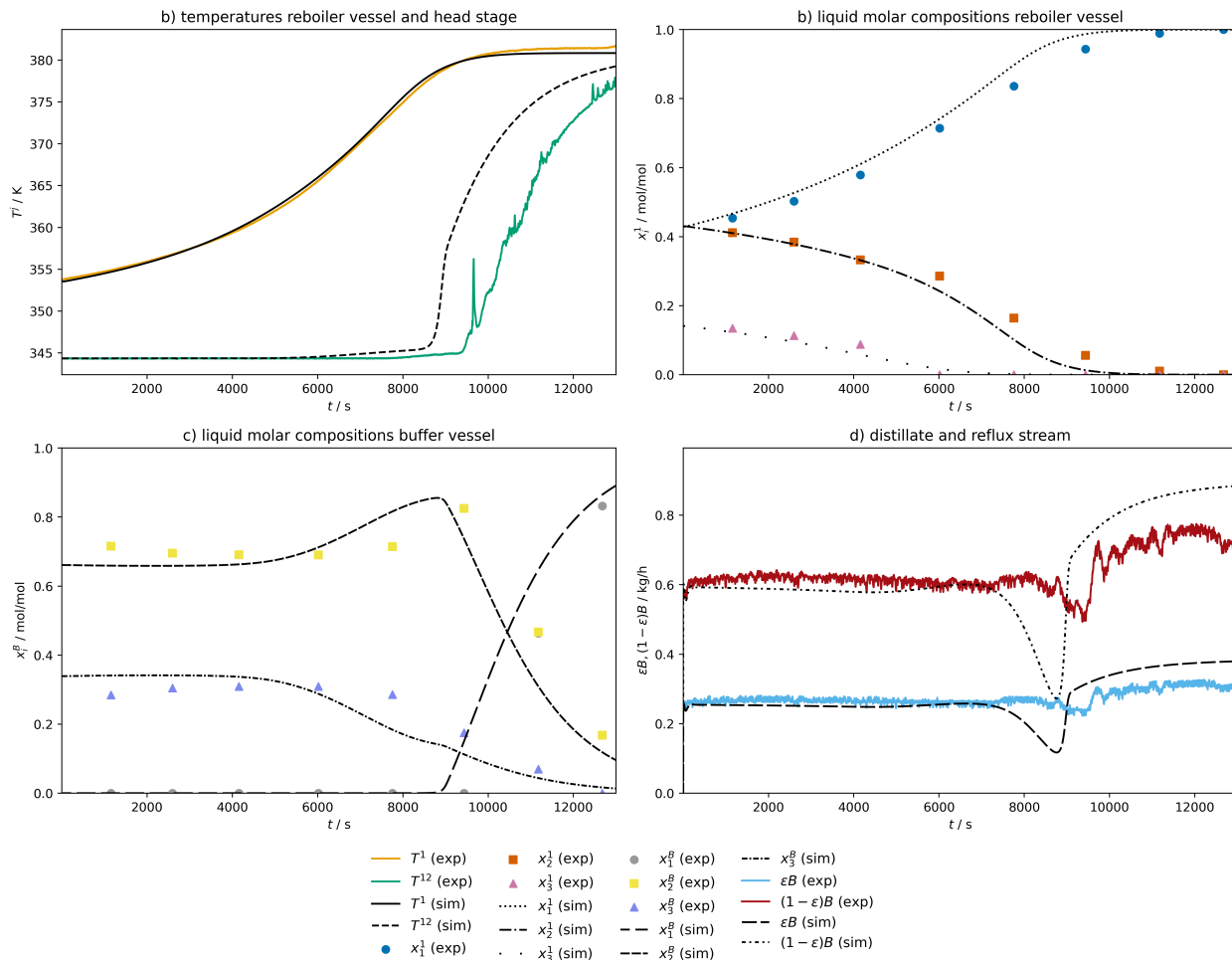


Figure 3: Comparison of experimental data (exp) and simulation results (sim) for the calibration experiment.

### 4.3 Examples for the prediction of fault-free experiments

Figure 4 compares model predictions with experimental data for a fault-free experiment. The conditions differ markedly from those of the calibration experiment; in particular, the heat duty was significantly lower, cf. Table 1. No adjustments to the plant-specific parameters determined for the calibration experiment (cf. Section 4.2) were made; the simulation results shown in Figure 4 are true predictions. The dynamic behavior is well captured, particularly with respect to the compositions. Nevertheless, some quantitative discrepancies remain, especially towards the end of the experiment. Overall, the quality of the predictions is comparable to that of the calibration experiment, indicating the robustness of the model.

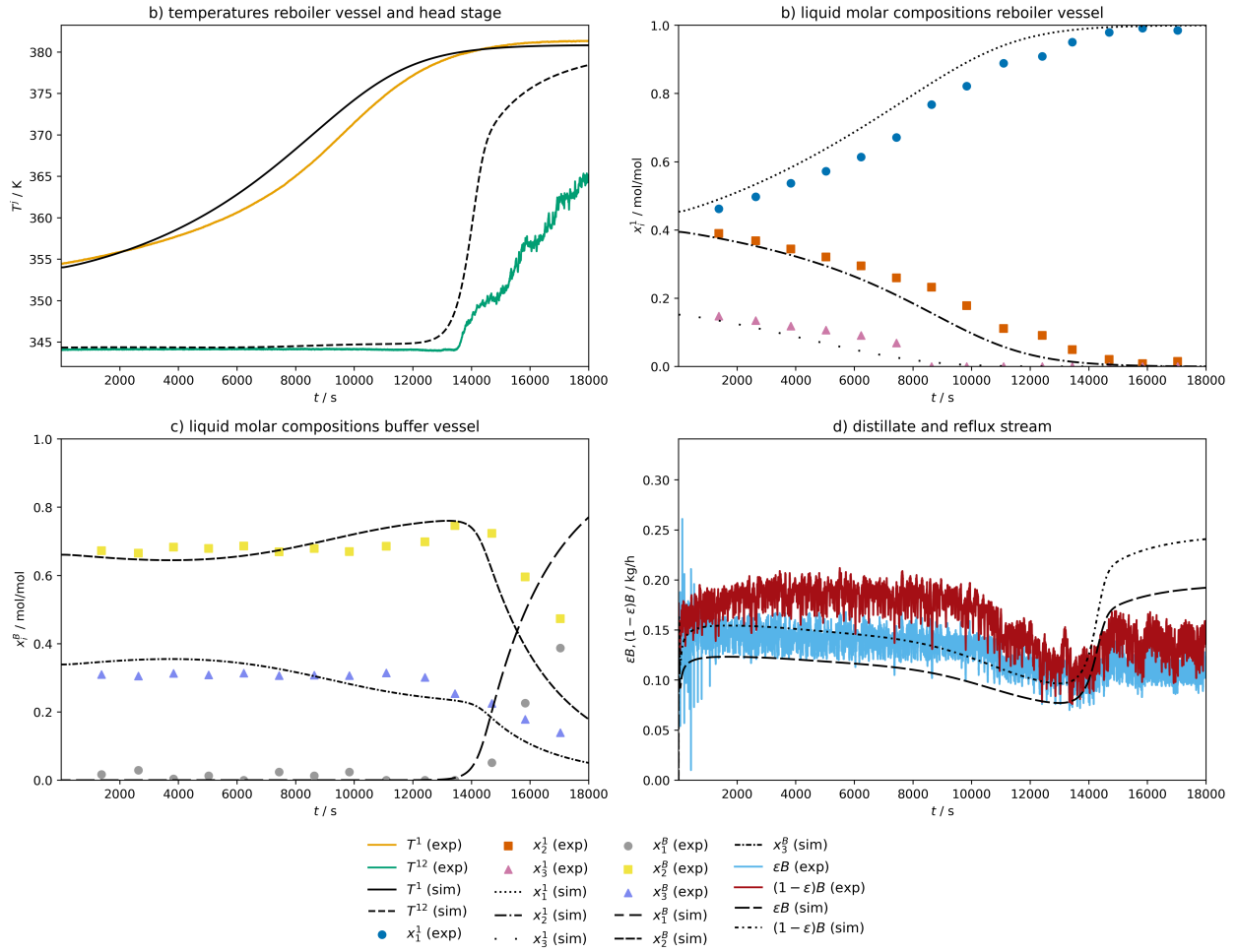


Figure 4: Comparison of experimental data (exp) and simulation results (sim) for a fault-free experiment, which was not used for adjusting the simulation model.

## 4.4 Examples for the prediction of anomalous experiments

### 4.4.1 Anomaly induced by efflux-ratio perturbations

We now discuss an experiment in which the efflux ratio was deliberately perturbed by two step changes, as shown in Figure 5, panel a). The remaining panels of Figure 5 compare the predicted temperatures of the reboiler vessel and column top, concentrations in the buffer vessel, and flow rates of distillate and reflux stream with the corresponding experimental data. The unperturbed operation is captured well overall, although some quantitative deviations persist in individual cases. The model also predicts the system's response to the perturbations well. Again, trends are predicted reliably, while residual quantitative discrepancies remain, as expected given that no adjustments to the plant-specific parameters determined for the calibration experiment (cf. Section 4.2) were made.

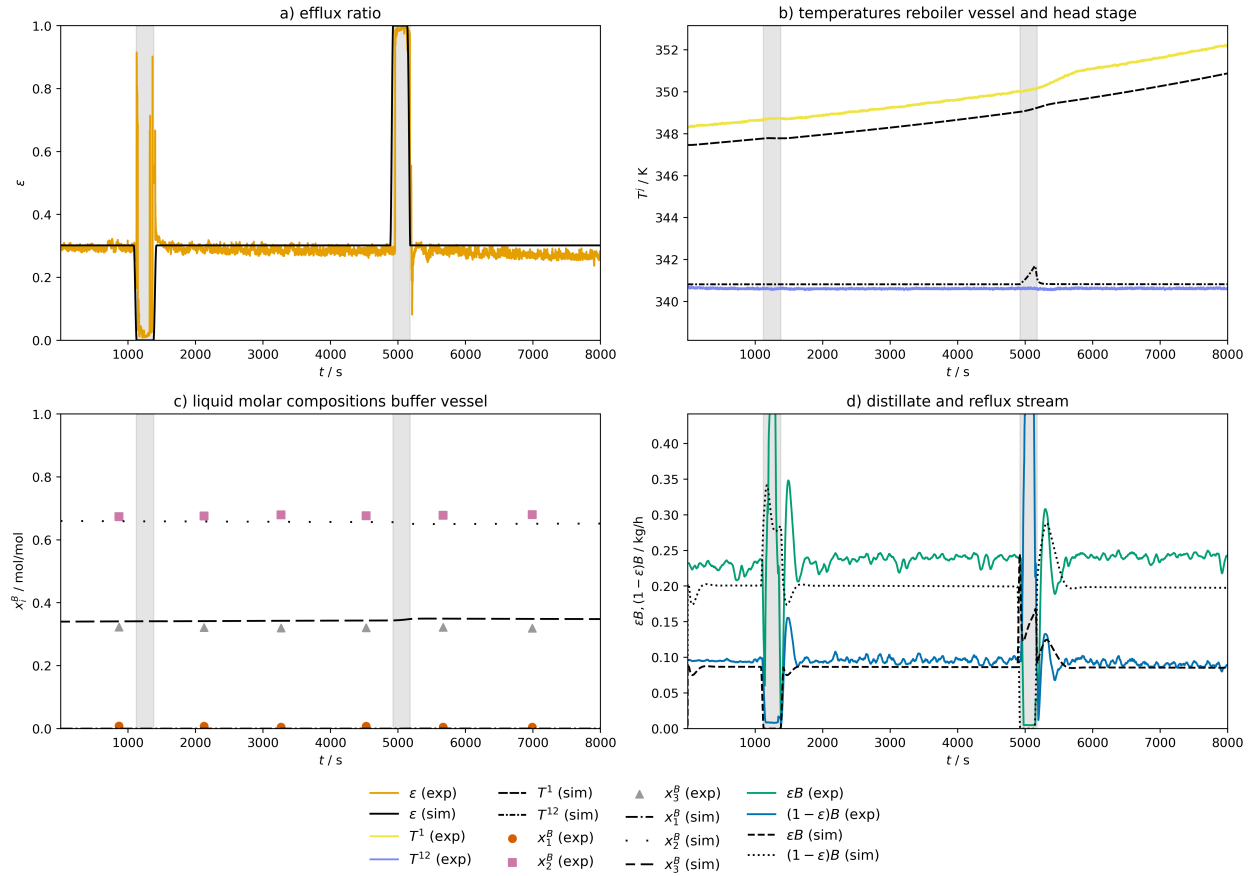


Figure 5: Comparison of experimental data (exp) and simulation results (sim) for an experiment with efflux-ratio perturbations (gray shaded regions mark the perturbation period during the simulation), which was not used for adjusting the simulation model.

#### 4.4.2 Anomaly induced by heat duty perturbation

We now discuss an experiment in which the heat duty was deliberately perturbed in two steps, as shown in Figure 6, panel a). The remaining panels of Figure 6 predicted temperatures of the reboiler vessel and column top, concentrations in the buffer vessel, and flow rates of distillate and reflux stream with the corresponding experimental data. The unperturbed operation is captured well overall, although some quantitative deviations persist. The model also accurately predicts the system's response to perturbations. Again, the trends are reliably predicted, but quantitative discrepancies remain, especially in the reboiler vessel temperature. As before, no further adjustments to the plant-specific parameters determined for the calibration (cf. Section 4.2) experiment were made.

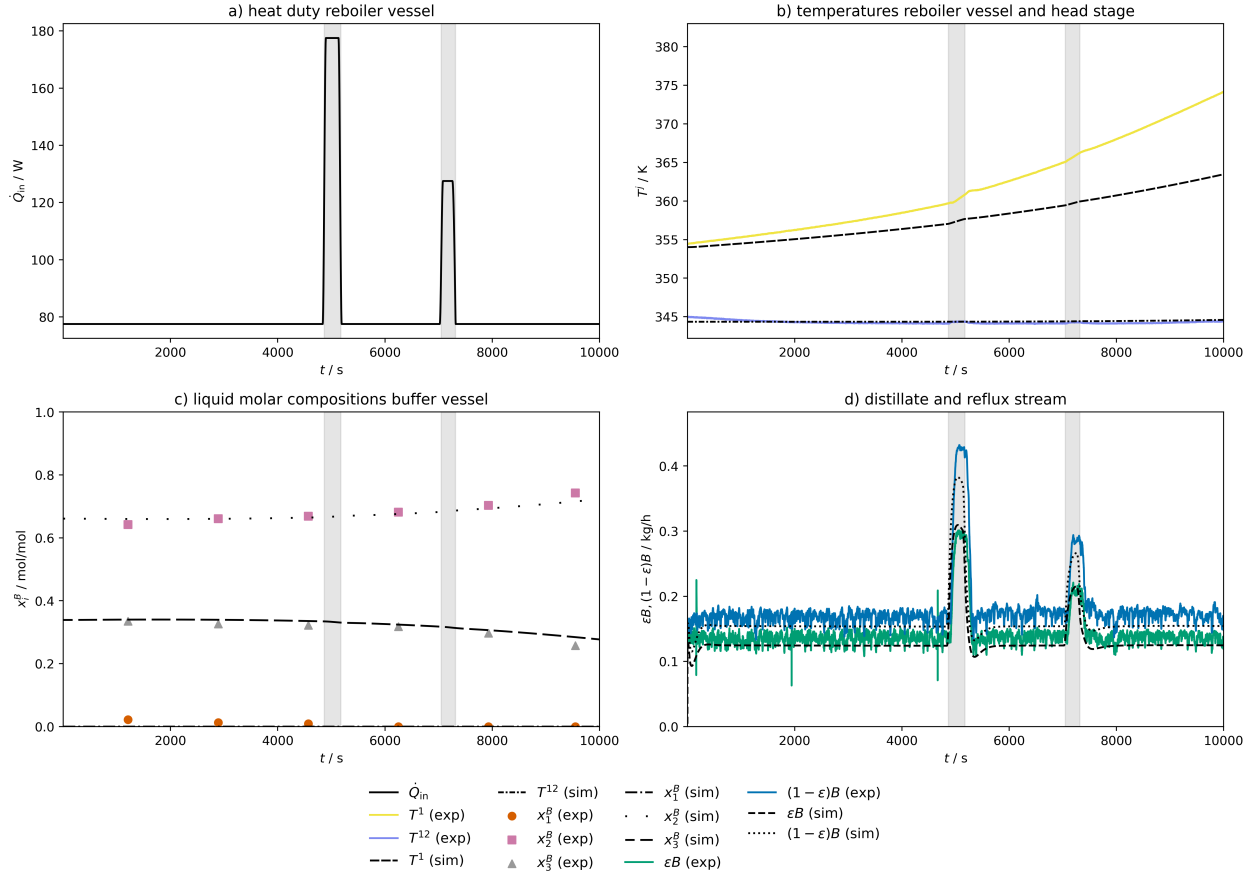


Figure 6: Comparison of simulation results (sim) and experimental data (exp) (except for the heat duty (panel a)) for an experiment with heater perturbation (gray shaded regions mark the perturbation period during the simulation), which was not used for adjusting the simulation model

#### 4.4.3 Anomaly induced by pressure-control perturbation

Here, we discuss an experiment in which the column pressure control was deliberately perturbed, as shown in Figure 7, panel a). The remaining panels of Figure 7 compare the predicted temperatures of the reboiler vessel and column top, concentrations in the buffer vessel, and flow rates of distillate and reflux stream with the corresponding experimental data. The unperturbed operation is captured well overall, although some quantitative deviations persist. There are deviations in the system's response to the perturbations, as the pressure controller is not modeled, and the pressure could only be modeled as changing more slowly due to numerical limitations, deviates slightly from the experiment. Moreover, the recovery after the perturbation is not accurately depicted in the simulation because the pressure controller behavior of the batch distillation plant was not modeled. Still, the trends are reliably predicted, with the largest deviations occurring in the prediction of mass flows.

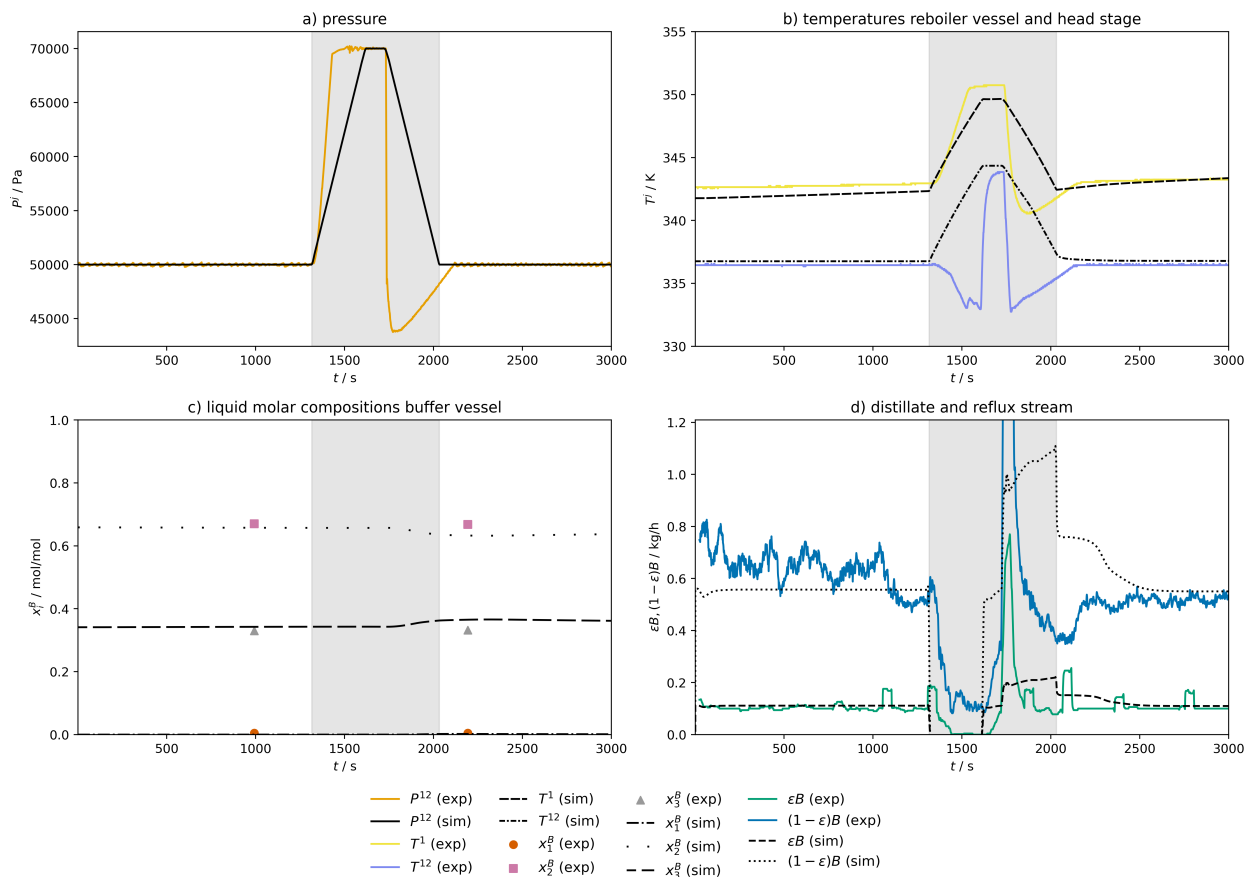


Figure 7: Comparison of experimental data (exp) and simulation results (sim) for an experiment with pressure-control perturbation (gray shaded regions mark the perturbation period during the simulation), which was not used for adjusting the simulation model.

#### 4.5 Simulation data within the hybrid dataset

The simulation data, including configuration files and comparisons to the experimental data, were added to the batch distillation database introduced in [19], creating a large hybrid database of experimental and simulation data. This hybrid database is published on <https://zenodo.org/records/17395543>, version 1.0.3, as an extension to the batch distillation database, which is organized as shown in Figure 8. In the main folder for the batch distillation plant data, all data modalities, including the novel simulation data modalities, are subsumed. On the next lower level, different combinations of plant setups and chemical systems are distinguished; on the second lowest level, operating points are distinguished. The actual simulation configuration files and time-series simulation data can be found on the lowest level of their respective folder tree.

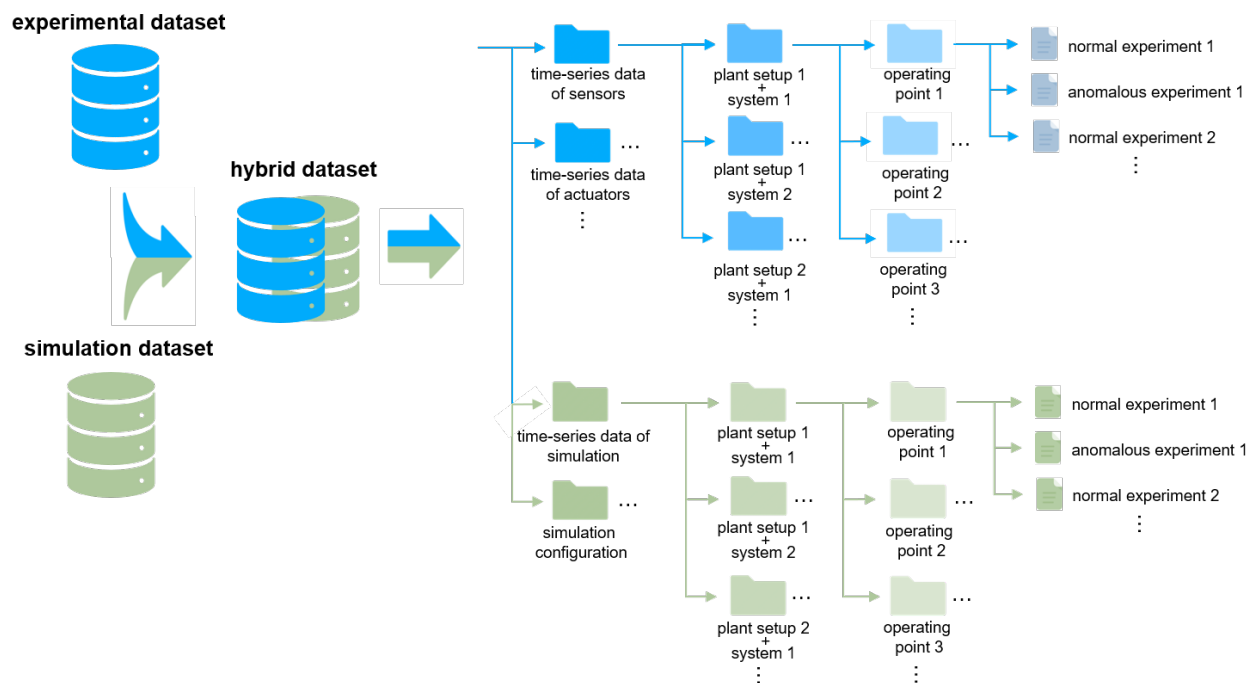


Figure 8: Overview of the extension of the experimental database [19] with the simulation data from this work. The hierarchy level decreases from left to right. The top-level folders represent the additional modalities of the simulated datasets, which are included in the same main set as the experimental data from [19], while the actual data are stored at the lowest level.

The configuration files consist of two .xml files; one contains all model parameters for pure-component properties, which cannot be made public, and binary interactions. The other contains all plant and process control parameters and includes a mapping to the anomaly identifiers from [19], indicating whether the respective anomalies of an experiment are simulated. In the hybrid database we only report the configuration file containing plant and process control parameters, binary interaction parameters are reported in the Supporting Information. An example of an .xml configuration file for an anomalous process is provided in the Supporting Information. Each simulated time series consists of features for liquid molar holdup, vapor up-flow, liquid down-flow, enthalpies and pressures per stage, for liquid mole fractions and vapor mole fractions per stage and component and for heat duty, efflux ratio, and fluxes of distillate and reflux streams. The simulation of each experiment extends the distillation process at least as far as the actual experiment did; if feasible, the simulation was run until the reboiler vessel was empty.

## 5 Conclusions

Large, diverse, and well-annotated datasets are a key prerequisite for training and benchmarking deep anomaly detection (AD) methods for chemical processes. Building on a recently released experimental batch distillation database with structured anomaly annotations, this work adds a consistent simulation layer, thereby creating an openly available hybrid dataset that combines experimental and simulated time-series data.

From a process-simulation perspective, we demonstrate that a laboratory-scale batch distillation campaign can be simulated in a largely automated and physically consistent manner. Using the metadata from the experimental database, initial and operating conditions are automatically retrieved and translated into simulation scenarios. After calibration to a single reference experiment, the simulator predicts the dynamics of the remaining experiments across a wide range of conditions. The developed workflow enables systematic “replay” simulations of confirmed anomalies with known causes. At the same time, open gaps in anomaly simulation remain: we only considered anomalies

induced by perturbations that can be modeled straightforwardly, such as set-point changes. The modeling of other anomalies, for example, those caused by foaming, remains an open challenge for future research.

From an AD perspective, the hybrid dataset provides two complementary benefits. First, it extends the experimental database with simulated trajectories for most runs, enabling controlled comparisons between measurements and physically consistent model outputs. Second, it enables the generation of additional pseudo-experimental data at low cost—both by exploring operating conditions and fault scenarios that are impractical or undesirable to realize experimentally and by creating larger and more diverse training corpora than would be feasible from experiments alone. Fully exploiting this potential, however, requires bridging the gap between simulated data and experimental data that contain noise, sensor errors, failures, and various inconsistencies. Machine learning provides techniques for such simulation-to-experiment translation (e.g., style transfer), which can now be systematically tested and refined based on the released hybrid dataset.

Experimental and simulated data overlap only partially: the overlap is valuable for validation and for learning mappings between domains, while the simulation domain additionally provides access to fully specified, internally consistent state and parameter information that is not directly observable in experiments. This combination motivates future work to better leverage simulated data for robust learning-based AD. Overall, the presented simulator and workflow, together with the released hybrid dataset, provide a practical basis for developing, testing, and comparing deep AD methods on chemical-process time series at a scale that is difficult to achieve experimentally.

## Acknowledgements

The authors gratefully acknowledge funding from the Deutsche Forschungsgemeinschaft (DFG), through the DFG Research Unit FOR 5359 “Deep Learning on Sparse Chemical Process Data” (grant number 459419731).

## Conflicts of interest

There are no conflicts of interest to declare.

## Author contributions

Jennifer Werner: Conceptualization, Software, Validation, Investigation, Data curation, Writing – original draft, Visualization. Justus Arweiler: Conceptualization, Investigation, Validation, Writing – original draft, Data curation, Visualization. Indra Jungjohann: Conceptualization, Investigation, Validation, Writing – original draft, Data curation, Visualization. Jochen Schmid: Conceptualization, Methodology, Formal analysis, Validation, Investigation, Writing – original draft, Supervision. Fabian Jirasek: Conceptualization, Writing – review & editing, Supervision, Project administration, Funding acquisition. Hans Hasse: Conceptualization, Writing – review & editing, Supervision, Project administration, Funding acquisition. Michael Bortz: Conceptualization, Resources, Writing – review & editing, Supervision, Project administration, Funding acquisition.

## Code availability statement

As parts of the code were developed in industrial collaborations, it cannot currently be released openly; however, interested users are encouraged to contact the authors to discuss possible forms of access.

## References

- [1] V. Chandola, A. Banerjee, V. Kumar, Anomaly detection: A survey, *ACM Comput. Surv.* 41 (3) (2009) 1–58. doi:10.1145/1541880.1541882.
- [2] V. Venkatasubramanian, R. Rengaswamy, K. Yin, S. N. Kavuri, A review of process fault detection and diagnosis part i: Quantitative model-based methods, *Comput. Chem. Eng.* 27 (3) (2003) 293–311. doi:10.1016/s0098-1354(02)00160-6.
- [3] V. Venkatasubramanian, R. Rengaswamy, S. N. Kavuri, A review of process fault detection and diagnosis part ii: Qualitative models and search strategies, *Comput. Chem. Eng.* 27 (3) (2003) 313–326. doi:10.1016/s0098-1354(02)00161-8.
- [4] V. Venkatasubramanian, R. Rengaswamy, S. N. Kavuri, K. Yin, A review of process fault detection and diagnosis part iii: Process history based methods, *Comput. Chem. Eng.* 27 (3) (2003) 327–346. doi:10.1016/s0098-1354(02)00162-x.
- [5] L. H. Chiang, *Fault Detection and Diagnosis in Industrial Systems*, Advanced Textbooks in Control and Signal Processing, Springer, London, 2001.
- [6] F. Hartung, B. J. Franks, T. Michels, D. Wagner, P. Liznerski, S. Reithermann, S. Fellenz, F. Jirasek, M. Rudolph, D. Neider, H. Leitte, C. Song, B. Kloepper, S. Mandt, M. Bortz, J. Burger, H. Hasse, M. Kloft, Deep anomaly detection on tennessee eastman process data, *Chem. Ing. Tech.* 95 (7) (2023) 1077–1082. doi:10.1002/cite.202200238.
- [7] D. Wagner, T. Michels, F. C. Schulz, A. Nair, M. Rudolph, M. Kloft, Timesead: Benchmarking deep multivariate time-series anomaly detection, *Trans. Mach. Learn. Res.* (2023). URL <https://openreview.net/forum?id=iMmsCI0JsS>
- [8] E. L. Russell, L. H. Chiang, R. D. Braatz, *Data-driven Methods for Fault Detection and Diagnosis in Chemical Processes*, Springer London, 2000. doi:10.1007/978-1-4471-0409-4.
- [9] I. Monroy, G. Escudero, M. Graells, Anomaly detection in batch chemical processes, in: 19th European Symposium on Computer Aided Process Engineering, Elsevier, 2009, pp. 255–260. doi:10.1016/s1570-7946(09)70043-4.
- [10] J. Inoue, Y. Yamagata, Y. Chen, C. M. Poskitt, J. Sun, Anomaly detection for a water treatment system using unsupervised machine learning, in: 2017 IEEE International Conference on Data Mining Workshops (ICDMW), IEEE, 2017, pp. 1058–1065. doi:10.1109/icdmw.2017.149.
- [11] G. S. Chadha, A. Rabbani, A. Schwung, Comparison of semi-supervised deep neural networks for anomaly detection in industrial processes, in: 2019 IEEE 17th International Conference on Industrial Informatics (INDIN), IEEE, 2019, pp. 214–219. doi:10.1109/indin41052.2019.8972172.
- [12] B. Song, Y. Suh, Narrative texts-based anomaly detection using accident report documents: The case of chemical process safety, *J. Loss Prev. Process Ind.* 57 (2019) 47–54. doi:10.1016/j.jlp.2018.08.010.
- [13] W. Tian, Z. Liu, L. Li, S. Zhang, C. Li, Identification of abnormal conditions in high-dimensional chemical process based on feature selection and deep learning, *Chinese J. Chem. Eng.* 28 (7) (2020) 1875–1883. doi:10.1016/j.cjche.2020.05.003.
- [14] S. Schmidl, P. Wenig, T. Papenbrock, Anomaly detection in time series: a comprehensive evaluation, *Proceedings of the VLDB Endowment* 15 (9) (2022) 1779–1797. doi:10.14778/3538598.3538602.

- [15] G. Wu, Y. Zhang, L. Deng, J. Zhang, T. Chai, Cross-modal learning for anomaly detection in complex industrial process: Methodology and benchmark, arXiv (2024). doi:10.48550/ARXIV.2406.09016.
- [16] Z. Zamanzadeh Darban, G. I. Webb, S. Pan, C. Aggarwal, M. Salehi, Deep learning for time series anomaly detection: A survey, *ACM Comput. Surv.* 57 (1) (2024) 1–42. doi:10.1145/3691338.
- [17] J. Downs, E. Vogel, A plant-wide industrial process control problem, *Comput. Chem. Eng.* 17 (3) (1993) 245–255. doi:10.1016/0098-1354(93)80018-i.
- [18] C. A. Rieth, B. D. Amsel, R. Tran, M. B. Cook, Additional tennessee eastman process simulation data for anomaly detection evaluation, *Harvard Dataverse* (2017). doi:10.7910/DVN/6C3JR1.
- [19] J. Arweiler, I. Jungjohann, A. Muraleedharan, H. Leitte, J. Burger, K. Münnemann, F. Jirasek, H. Hasse, Batch distillation data for developing machine learning anomaly detection methods, *Sci. Data* 13 (513) (2026). doi:10.1038/s41597-026-07124-3.
- [20] A. Muraleedharan, A. Ferre, J. Arweiler, I. Jungjohann, F. Jirasek, H. Hasse, J. Burger, Experimental time series data with and without anomalies from a continuous distillation mini-plant for development of machine learning anomaly detection methods *EngrXiv preprint* (2025). doi:10.31224/5631.  
URL <https://engrxiv.org/preprint/view/5631>
- [21] D. Wagner, F. Hartung, J. Arweiler, A. Muraleedharan, I. Jungjohann, A. Nair, S. Reithermann, R. Schulz, M. Bortz, D. Neider, H. Leitte, J. Pfeffinger, S. Mandt, S. Fellenz, T. Katz, F. Jirasek, J. Burger, H. Hasse, M. Kloft, Noboom: Chemical process datasets for industrial anomaly detection, *NeurIPS 2025 Datasets and Benchmarks* (2025).  
URL <https://openreview.net/forum?id=qiLboR0ocm>
- [22] C. Ji, W. Sun, A review on data-driven process monitoring methods: Characterization and mining of industrial data, *Processes* 10 (2) (2022). doi:10.3390/pr10020335.
- [23] Y.-J. Park, S.-K. S. Fan, C.-Y. Hsu, A review on fault detection and process diagnostics in industrial processes, *Processes* 8 (9) (2020). doi:10.3390/pr8091123.
- [24] U. M. Ascher, L. R. Petzold, *Computer methods for ordinary differential equations and differential-algebraic equations*, SIAM, 1998.
- [25] E. Hairer, G. Wanner, *Solving ordinary differential equations II: Stiff and differential-algebraic problems*, Springer Berlin Heidelberg, 1991. doi:10.1007/978-3-642-05221-7.
- [26] P. Kunkel, *Differential-algebraic equations: analysis and numerical solution*, Vol. 2, European Mathematical Society, 2006.
- [27] S. Campbell, A. Ilchmann, V. Mehrmann, T. Reis, *Applications of Differential-Algebraic Equations: Examples and Benchmarks*, Springer, 2019. doi:10.1007/978-3-030-03718-5.
- [28] M. Doherty, J. Perkins, On the dynamics of distillation processes—I: The simple distillation of multicomponent non-reacting, homogeneous liquid mixtures, *Chem. Eng. Sci.* 33 (3) (1978) 281–301. doi:10.1016/0009-2509(78)80086-4.
- [29] D. B. Van Dongen, M. F. Doherty, On the dynamics of distillation processes—vi. batch distillation, *Chem. Eng. Sci.* 40 (11) (1985) 2087–2093. doi:10.1016/0009-2509(85)87026-3.

- [30] R. Bachmann, L. Brüll, T. Mrziglod, U. Pallaske, On methods for reducing the index of differential algebraic equations, *Comput. Chem. Eng.* 14 (11) (1990) 1271–1273. doi:10.1016/0098-1354(90)80007-X.
- [31] Aspen Plus®<sup>®</sup>, Version 15, process simulation software (2025).
- [32] J. Haydary, *Chemical Process Design and Simulation: Aspen Plus and Aspen Hysys Applications*, Wiley, 2018. doi:10.1002/9781119311478.
- [33] A. Cervantes, L. T. Biegler, Large-scale dae optimization using a simultaneous nlp formulation, *AIChE J.* 44 (5) (1998) 1038–1050. arXiv:https://aiche.onlinelibrary.wiley.com/doi/pdf/10.1002/aic.690440505, doi:10.1002/aic.690440505.
- [34] A. M. Cervantes, A. Wächter, R. H. Tütüncü, L. T. Biegler, A reduced space interior point strategy for optimization of differential algebraic systems, *Comput. Chem. Eng.* 24 (1) (2000) 39–51. doi:10.1016/S0098-1354(00)00302-1.
- [35] A. M. Cervantes, L. T. Biegler, A stable elemental decomposition for dynamic process optimization, *J. Comput. Appl. Math.* 120 (1) (2000) 41–57. doi:10.1016/S0377-0427(00)00302-2.
- [36] L. T. Biegler, A. M. Cervantes, A. Wächter, Advances in simultaneous strategies for dynamic process optimization, *Chem. Eng. Sci.* 57 (4) (2002) 575–593. doi:10.1016/S0009-2509(01)00376-1.
- [37] A. U. Raghunathan, M. Soledad Diaz, L. T. Biegler, An MPEC formulation for dynamic optimization of distillation operations, *Comput. Chem. Eng.* 28 (10) (2004) 2037–2052, special Issue for Professor Arthur W. Westerberg. doi:10.1016/j.compchemeng.2004.03.015.
- [38] S. Gruetzmann, T. Kapala, G. Fieg, Dynamic modelling of complex batch distillation starting from ambient conditions, in: *16th European Symposium of Computer Aided Process Engineering and 9th International Symposium on Process Systems Engineering*, 2006.
- [39] E. Eckert, T. Vaněk, Mathematical modelling of selected characterisation procedures for oil fractions, *Chem. Pap.* 62 (2008) 26–33.
- [40] E. S. Lopez-Saucedo, I. E. Grossmann, J. G. Segovia-Hernandez, S. Hernández, Rigorous modeling, simulation and optimization of a conventional and nonconventional batch reactive distillation column: A comparative study of dynamic optimization approaches, *Chem. Eng. Res. Des.* 111 (2016) 83–99.
- [41] E. S. Lopez-Saucedo, I. E. Grossmann, J. G. Segovia-Hernandez, S. Hernández, Rigorous modeling, simulation and optimization of a conventional and nonconventional batch reactive distillation column: A comparative study of dynamic optimization approaches, *Chem. Eng. Res. Des.* 111 (2016) 83–99. doi:10.1016/j.cherd.2016.04.005.
- [42] M. Bortz, R. Heese, A. Scherrer, T. Gerlach, T. Runowski, Estimating mixture properties from batch distillation using semi-rigorous and rigorous models, in: *Comput. Aided Chem. Eng.*, Vol. 46, Elsevier, 2019, pp. 643–648. doi:10.1016/B978-0-12-818634-3.50108-9.
- [43] J. Mohring, J. Schmid, J. Wlazło, R. Heese, T. Gerlach, T. Kochenburger, M. Bortz, Modeling and optimizing dynamic networks: Applications in process engineering and energy supply, in: M. Bortz, N. Asprion (Eds.), *Simulation and Optimization in Process Engineering*, Elsevier, 2022, pp. 143–160. doi:10.1016/B978-0-323-85043-8.00013-1.
- [44] X. Qian, K.-H. Lin, S. Jia, L. T. Biegler, K. Huang, Nonlinear model predictive control for dividing wall columns, *AIChE J.* 69 (6) (2023) e18062. doi:10.1002/aic.18062.

- [45] J. Werner, J. Schmid, L. T. Biegler, M. Bortz, An equation-based batch distillation simulation to evaluate the effect of multiplicities in thermodynamic activity coefficients, *Fluid Phase Equilib.* 598 (2025) 114465. doi:10.1016/j.fluid.2025.114465.
- [46] L. A. Gatys, A. S. Ecker, M. Bethge, Image style transfer using convolutional neural networks, in: 2016 IEEE Conference on Computer Vision and Pattern Recognition (CVPR), 2016, pp. 2414–2423. doi:10.1109/CVPR.2016.265.
- [47] Y. El-Laham, S. Vyetenko, Styletime: Style transfer for synthetic time series generation, in: Proceedings of the Third ACM International Conference on AI in Finance, ICAIF '22, Association for Computing Machinery, New York, NY, USA, 2022, p. 489–496. doi:10.1145/3533271.3561772.
- [48] X. Xu, Z. Wang, Y. Zhang, Y. Liu, Z. Wang, Z. Xu, M. Zhao, H. Luo, Style transfer: From stitching to neural networks, in: 2024 5th International Conference on Big Data & Artificial Intelligence & Software Engineering (ICBASE), 2024, pp. 526–530. doi:10.1109/ICBASE63199.2024.10762296.
- [49] M. Nagda, P. Ostheimer, J. Arweiler, I. Jungjohann, J. Werner, D. Wagner, A. Muraleedharan, P. Jafari, J. Schmid, F. Jirasek, J. Burger, M. Bortz, H. Hasse, S. Mandt, M. Kloft, S. Fellenz, Diffstylets: Diffusion model for style transfer in time series (2025). arXiv:2510.11335, doi:10.48550/arXiv.2510.11335.
- [50] W. Schnelle, J. Engelhardt, E. Gmelin, Specific heat capacity of apiezon n high vacuum grease and of duran borosilicate glass, *Cryogenics* 39 (3) (1999) 271–275. doi:10.1016/S0011-2275(99)00035-1.
- [51] P. Pichler, B. Simonds, J. Sowards, G. Pottlacher, Measurements of thermophysical properties of solid and liquid nist srm 316l stainless steel, *J. Mater. Sci.* 55 (9) (2020) 4081–4093. doi:10.1007/s10853-019-04261-6.